Spectral characterization of soil and coal contamination on snow reflectance using hyperspectral analysis

S K Singh[1,*], A V Kulkarni[1] and B S Chaudhary[2]

[1]*Marine and Earth Sciences Group, Space Applications Centre (ISRO), Ahmedabad 380 015, India.*
[2]*Department of Geophysics, Kurukshetra University, Kurukshetra 136 119, India.*
[*]*e-mail: sushil@sac.isro.gov.in*

Snow is a highly reflecting object found naturally on the Earth and its albedo is highly influenced by the amount and type of contamination. In the present study, two major types of contaminants (soil and coal) have been used to understand their effects on snow reflectance in the Himalayan region. These contaminants were used in two categories quantitatively – addition in large quantity and addition in small quantity. Snow reflectance data were collected between 350 and 2500 nm spectral ranges and binned at 10 nm interval by averaging. The experiment was designed to gather the field information in controlled conditions, and radiometric observations were collected. First derivative, band absorption depth, asymmetry, percentage change in reflectance and albedo in optical region were selected to identify and discriminate the type of contamination. Band absorption depth has shown a subtle increasing pattern for soil contamination, however, it was significant for small amounts of coal contamination. The absorption peak asymmetry was not significant for soil contamination but showed a nature towards left asymmetry for coal. The width of absorption feature at 1025 nm was not significant for both the contaminations. The percentage change in reflectance was quite high for small amount of coal contamination rather than soil contamination, however, a shift of peak was observed in soil-contaminated snow which was not present in coal contamination. The albedo drops exponentially for coal contamination rather than soil contamination.

1. Introduction

Snow plays an important role in hydrological and climatic applications in mountainous regions. Field measurements of snow properties provide point observations but are restricted to limited locations due to rough terrain and harsh weather conditions. Remote sensing provides information about snow properties, which conventionally are not possible for a larger area due to typical terrain conditions. Snow shows high reflectance in visible wavelength region and low reflectance in Short Wave Infrared (SWIR) region. This spectral property of snow was used for snow cover monitoring on a regular basis using Moderate Resolution Imaging Spectroradiometer (MODIS) and Advance Wide field Sensor (AWiFS) sensors (Hall *et al* 1995, 2002; Kulkarni *et al* 2006).

Reflectance of fresh snow is approximately 90% in visible region and reduces at longer wavelengths. Freshly fallen snow almost immediately begins to compact and metamorphose, and this changes the snowpack characteristics. The albedo of fresh snow in the visible region of the spectrum remains high but decreases slowly with its age, but in the near-infrared region, the albedo of aging snow decreases considerably as compared to fresh snow (O'Brian and Munis 1975; Warren and Wiscombe 1980;

Keywords. Snow; hyperspectral; soil; coal; contamination; albedo.

Wiscombe and Warren 1981). Wiscombe and Warren (1981) have shown that minute concentrations of small highly absorbing particles can lower snow albedo in the visible wavelengths by 5–15%. Gerland *et al* (1999) measured a maximum albedo >90% on Svalbard, Norway, before melt onset, and 60% after melt progressed in the spring when the snow was considered old but still clean. Snow cover area, albedo, grain size, snow temperature, wetness and meteorological parameters are required for any snow melt run-off model.

In undulating terrain like the Himalayas, the atmospheric conditions change very fast specially in the lower Himalayan region. Temperature difference is significant during day and night which generates melt-freeze cycles. Very few studies have been carried out using field spectroradiometer to understand the snow characteristics in the Himalayan region. Spectroradiometer data of Beas basin was used in the present study. Contaminated snow shows a decrease in reflectance in visible region whereas grain size within snowpack has more influence in NIR region (Singh *et al* 2005, 2008). Contamination and effect of mixed objects like vegetation, soil on snow reflectance for Himalayan region was reported by Negi *et al* (2006, 2009) where different indices were attempted to provide an understanding of snow pixel identification under different scenarios for broadband sensors. Hyperspectral behaviour of soil contamination and grain size variability was studied using field-based data for selected bands in visible and SWIR regions. This study has shown a possibility of detection type of metamorphism using absorption peak behaviour at 1025 nm and percentage change in reflectance (Singh *et al* 2010). Increasing number of airborne/satellite hyperspectral sensors like Airborne Visible/Infrared Imaging Spectrometer (AVIRIS) and Hyperion provide an opportunity to measure absorption spectrum and its utilities to improve applications (Gao *et al* 1993; Price 1998). Dust and coal contamination are major source of contamination influencing the snow and glaciated region through avalanche and atmospheric phenomenon. Dust concentration in the snow cover revealed the sporadic high concentrations frequently in spring and large year-to-year variations in the amount deposited from winter to spring (Osada *et al* 2004). In the present study, two contaminants – soil and coal – were used as snow contamination to understand the effect of varying amount of contamination on snow reflectance. Hyperspectral techniques were also used to derive the information which could be helpful to identify/discriminate the type and amount of contamination.

2. Study area

Beas basin was selected as the study area for this experiment. It is in the Pir-Panjal range and altitude varies between 2000 and 4000 m. The study area can be characterized by moderate temperature and high precipitation. Snow fall takes place even in lower ridges of this basin and as the summer approaches, melting of snow takes place. Due to moderate temperature, the snow cover changes into isothermal snow pack at 0°C and the winter period remains short. Location map of the Beas basin is shown in figure 1. Snow and Avalanche Study

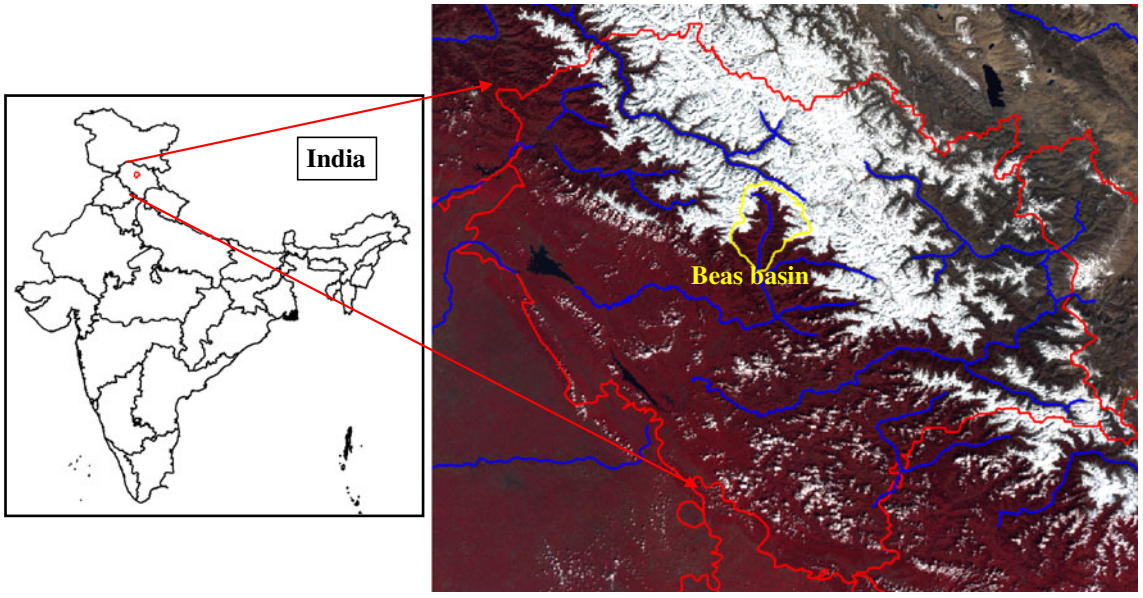

Figure 1. IRS AWiFS image superimposed with Beas basin boundaries.

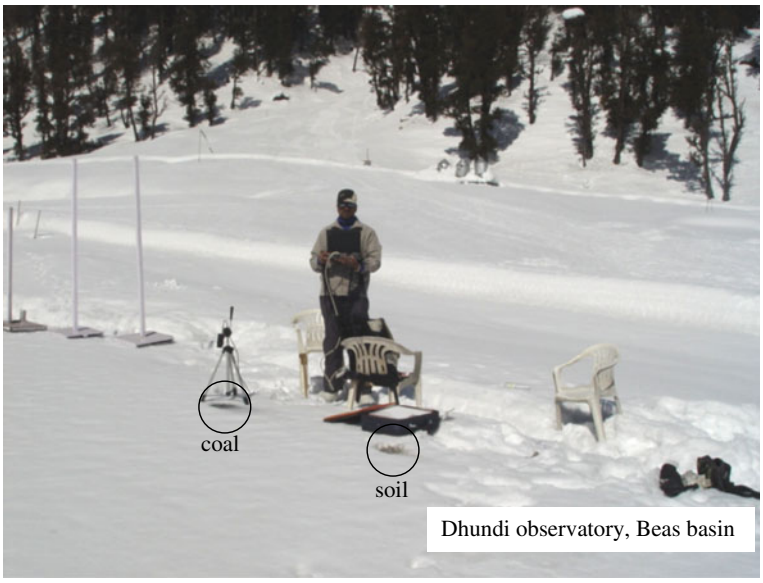

Figure 2. Field experiment setup for soil and coal contamination on snow reflectance.

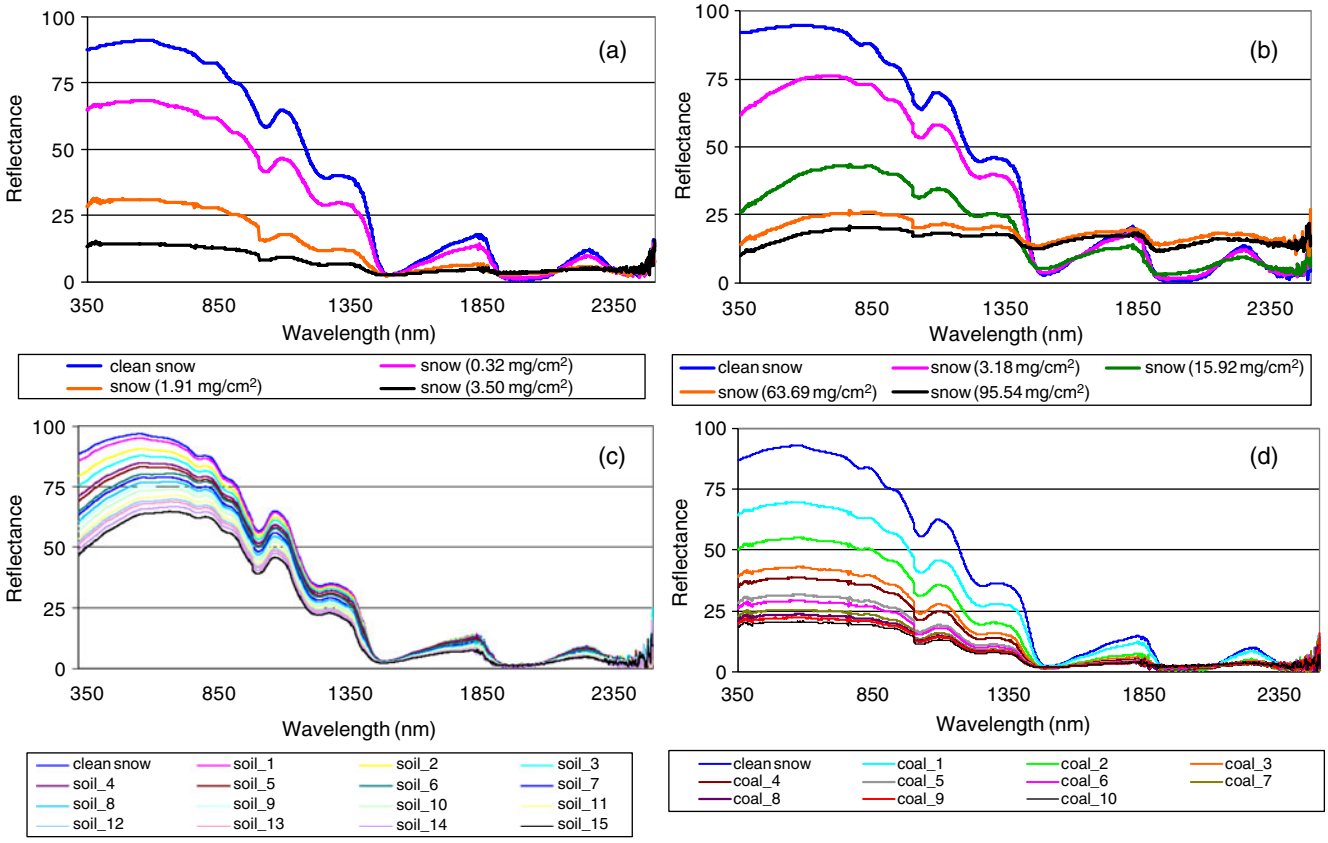

Figure 3. Soil and coal contaminated reflectance for (**a**) large addition of soil contamination, (**b**) large addition of coal contamination, (**c**) small addition of soil contamination (0.32 mg/cm^2 per packet), and (**d**) small addition of coal contamination (0.32 mg/cm^2 per packet).

Establishment (SASE) observatory, which was considered for the snow reflectance and other collateral data collection in the present study, is established at Dhundi (32.36°N; 77.13°E) (Mohile *et al* 2004). This observatory receives significant amount of seasonal snowfall on average between November and

April (Bahang – 53 cm, Solang – 127 cm and Dhundi – 219 cm) and temperature also remains high in this area (T_{max}: 21°C and T_{min}: –5.0°C) in comparison to the other ranges of the Himalayas (Mohile *et al* 2004).

3. Field setup and data collection

ASD spectroradiometer was used in the present study which measures the radiometric quantities like radiance, reflectance and irradiance in spectral range between 350 and 2500 nm. The instrument collects the data at spectral resolution of 3 nm in visible and NIR region, and 10–12 nm in the SWIR region. The bare fibre optic with 25° field of view was used in the present study. Figure 2 depicts the experimental setup of ASD instrument during the field investigations. Crystal gauge with magnifying glass was used for estimating grain size of snow. Thermometer was used for snow skin temperature and air temperature measurements.

4. Methodology

In the present study, two types of contaminants – soil and coal – were used in varying amount of contamination in two categories during the experiment; first – adding large amount of concentration and second – adding small quantity of concentration. During soil/coal contamination experiment, soil was dried, grinded and filtered restricting the size of contamination particles within 0.5 mm. The soil was weighed into 1 gm (low), 5 gm (medium), 20 gm (high) and 30 gm (very high) packets which were equally distributed over the study area. Coal was grinded and weighed into 0.1 gm (low), 0.6 gm (medium) and 1.1 gm (high) packets of coal to be sprayed. These packets were used in the first phase of experiment. This was targeted to study the large amount of contaminants addition and its effect on snow reflectance. For the second part, small packets were prepared to observe the subtle variations in snow reflectance due to contaminants addition. In this 0.1 gm packets were prepared for both soil and coal contaminations. While spraying the contamination over study area, enough precautions were taken to distribute contamination equally in instrument's view area. Proper care was taken for other atmospheric parameters like wind, ambient disturbance, etc., having negligible effect. Snow was moist in nature with density of 0.24 gm/cc and a grain size of 0.1–0.6 mm. The instrument sensor was kept at such a height which makes the view area on surface at 20 cm diameter. Sensor was targeted to collect the observations for clean snow, spraying soil and coal contaminants equally over the surface. Reflectance data was collected using bare fibre sensor (25° field of view) and approximately 15 measurements were collected to average out. The soil contamination was 0.0, 3.18, 15.92, 63.69 and 95.54 mg/cm^2 on the snow-covered surface (figure 3a). The coal contamination was 0.0, 0.32, 1.91 and 3.50 mg/cm^2 on the snow-covered surface (figure 3b). In the other experiment, small amounts of 0.1 gm (0.32 mg/cm^2) were prepared for both soil and coal experiments and sprayed over the targeted snow surface (figure 3c and d).

Measurement time of the experiment was from 1045–1245 h, however, duration of measurement was 10–15 minutes to avoid any other ambience introduction due to change in sun-sensor viewing geometrical and physical/meteorological conditions. Albedo was computed for each category of added soil contamination during the experiment. Study area has minimum human intervention which leads to an assumption of further minimization of any other effect. Field-based hyperspectral data was binned at 10 nm interval using simple averaging which is compatible to available hyperspectral satellite sensor's spectral resolution and also compatible with spectral resolution of field spectroradiometer at SWIR wavelengths, with the assumption of square wave response function.

The different wavelength regions were chosen based on the influence of physical change in the

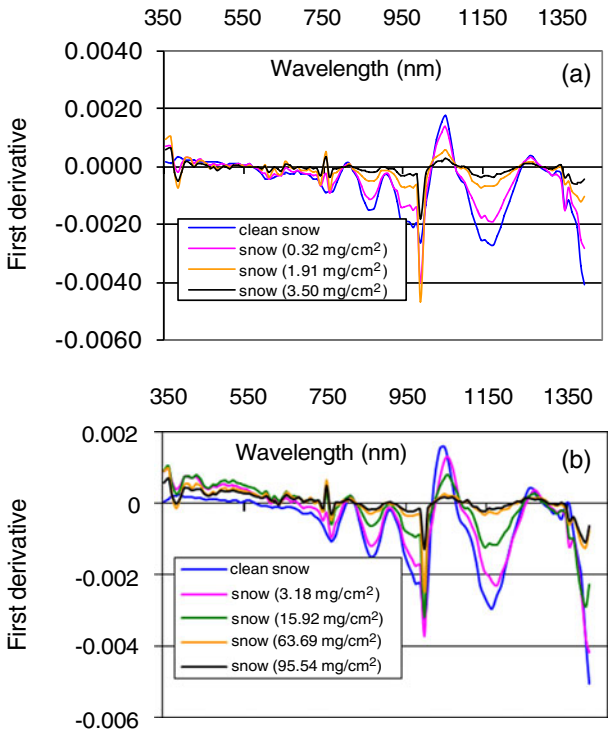

Figure 4. First derivative of (**a**) soil and (**b**) coal contamination on snow reflectance.

snowpack characteristics. Position, strength and shape of a spectral curve can provide the information on smoothly varying spectral properties. The absorption peak at 1025 nm was chosen in the study. Relative strength, width and asymmetry of the absorption feature were computed after continuum removal for different wavelength region. The objective of continuum removal is to isolate the properties of the absorption features from the overall reflectance properties. The relative strength of each band is computed using the following formula (Clark and Roush 1984):

$$S = \frac{(Rc - Rb)}{Rc}, \tag{1}$$

where S is the band strength, Rc is the reflectance of the continuum at the wavelength of Rb, and Rb the reflectance at the band minimum.

Band shape can be parameterized for the purposes of this systematic analysis by two simple parameters like full width at half maximum and asymmetry. The width of feature is the absolute difference in microns between the right and left sides of absorption, where the reflectance are half the strength of the band. Asymmetry is defined as the base 10 logarithm of the sum of the reflectance over the number of channels to the right of the band minimum divided by sum of the reflectance over the numbers of channels to the left of the band minimum. The zero value will represent perfectly symmetric band, +ve value for right asymmetry and –ve for left asymmetry. This parameterization allows a rapid reduction in the dimensionality of a spectroradiometer data to suite of key absorption feature.

$$\text{Asymmetry} = \log 10 \left(\frac{\sum R_{c\to\text{right}}}{\sum R_{\text{left}\to c}} \right), \tag{2}$$

where $R_{c\to\text{right}}$ represents the reflectance from centre to right and $R_{\text{left}\to c}$ represents the reflectance

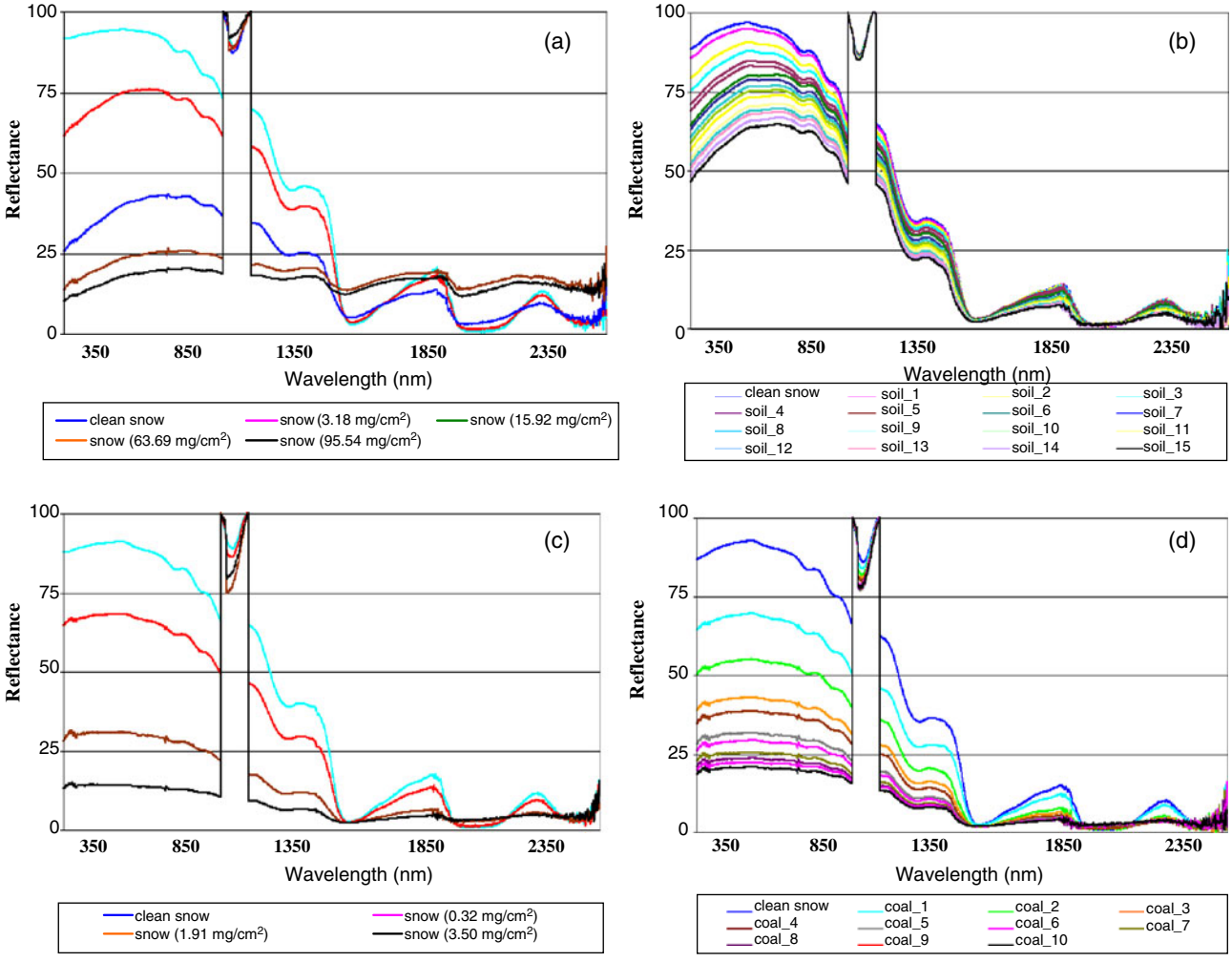

Figure 5. Continuum removal of (**a**) soil (large quantity); (**b**) soil (small quantity); (**c**) coal (large quantity); and (**d**) coal (small quantity) contaminated snow reflectance. This figure corresponds to continuum removal of figure 3.

from left to centre wavelength of the absorption peak. First and second derivatives were computed. First and second derivatives are helpful to provide any change in the shape of curve at particular wavelengths. The changes in percentage of reflectance were computed with contaminants. Correlation coefficient of the soil and coal contamination on snow reflectance was estimated. This information has been further used to identify the distinct spectral behaviour to identify the type of contamination based on identified bands. Difference of reflectance for soil and coal contamination was estimated and used to distinguish bands for contamination discrimination.

5. Results and discussion

The influence of soil and coal contamination on snow reflectance was studied with reference to its change on reflectance in the context of hyperspectral applications. Figure 3(a and b) shows the effect of soil and coal contamination on snow reflectance with high amount of concentration whereas a small quantity was used to observe the subtle changes of contamination on snow reflectance as shown in figure 3(c and d). Both contamination has large reduction in reflectance in visible region, however, the pattern changes in SWIR region. SWIR region has shown a reverse pattern for soil in comparison to soil contamination for higher amount of contamination. The diminish nature of snow peak in visible and NIR region can be observed in soil wherever reflectance almost flattens for coal contamination as also can be observed for small quantity addition of contamination (figure 3c and d). First derivative (FD) of soil and coal contamination for higher amount of contamination has been shown in figure 4(a) and 4(b), respectively. A shift in peak in visible region can be observed for soil contamination which is not present for coal contamination.

Figure 5(a and b) shows the relative strength of absorption peak at 1025 nm wavelength for high and small quantity of soil contamination, and figure 5(c and d) shows same for coal contamination. A decrease in relative strength can be observed for both contaminations however coal has shown large influence compared to soil as shown in figure 5(a and c). Decrease in relative strength for small quantity is not significant for soil; however, coal has a definite pattern of reduction at 1025 nm absorption peak. Figure 6(a) shows that absorption depth at 1025 nm for soil increases gently whereas for coal it increases rapidly. However, absorption depth at 1000 nm is almost unchanged for soil contamination but reduces for coal contamination. Figure 6(b) shows the right asymmetry unchanged

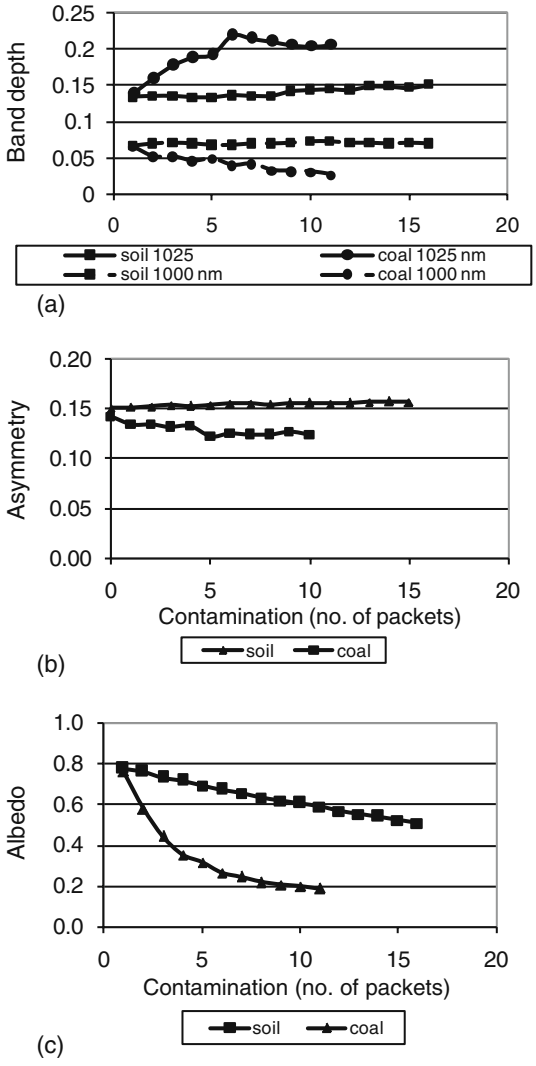

Figure 6. Soil and coal contamination for small quantity; (**a**) absorption band depth; (**b**) asymmetry at 1025 nm; and (**c**) effect on albedo.

for small quantity addition of soil contamination; however, coal has shown a slight left shift in asymmetricity of absorption curve at 1025 nm. Band width at 1025 nm has not shown any significant information for soil and coal contamination.

Table 1 shows that change in percentage reflectance which is not same at all wavelengths ranging from 350 to 2500 nm. The percentage change was estimated at six selected wavelengths. Soil contamination has shown approximately similar amount of reduction in reflectance from 575 to 1085 nm at different levels and has shown a reverse pattern for high contamination levels. Coal contamination has shown approximately close amount of reduction in reflectance from 575 to 745 nm. SWIR region has shown a large amount of reduction in reflectance as compared to reverse pattern observed in soil contamination. Figure 6(c) shows

Table 1. *Percentage change in reflectance for soil and coal contamination.*

Wavelength (nm)	Reflectance					Percentage change in reflectance			
	Clean snow	Low	Medium	High	Very high	Low	Medium	High	Very high
Soil contamination									
575	0.9458	0.7478	0.3984	0.2338	0.1788	20.93	57.88	75.28	81.09
585	0.9460	0.7507	0.4025	0.2365	0.1809	20.64	57.45	75.00	80.88
695	0.9349	0.7607	0.4270	0.2533	0.1960	18.63	54.33	72.91	79.04
745	0.9185	0.7539	0.4305	0.2570	0.2000	17.92	53.14	72.02	78.23
1085	0.6996	0.5816	0.3451	0.2155	0.1815	16.87	50.68	69.20	74.06
1645	0.1067	0.1066	0.1011	0.1788	0.1656	0.09	5.28	−67.55	−55.20
2265	0.1274	0.1155	0.0913	0.1754	0.1570	9.28	28.34	−37.69	−23.27
Coal contamination									
575	0.9128	0.6848	0.3116	0.1430		24.98	65.86	84.33	
585	0.9126	0.6846	0.3114	0.1430		24.98	65.88	84.33	
695	0.8814	0.6610	0.3003	0.1373		25.00	65.93	84.42	
745	0.8641	0.6475	0.2928	0.1344		25.07	66.11	84.45	
1085	0.6478	0.4660	0.1770	0.0923		28.07	72.68	85.76	
1645	0.0934	0.0775	0.0455	0.0358		17.04	51.31	61.64	
2265	0.1133	0.0929	0.0525	0.0482		17.98	53.61	57.46	

that albedo due to small quantity of soil contamination has a gradual decrease whereas an exponential decrease was observed for coal contamination.

6. Conclusions

Radiometric data for different levels of soil contamination and coal contamination were collected in controlled conditions in Himalayan region. Relative strength, asymmetry, first derivative, percentage change in reflectance and albedo were used to analyze the field data. Relative strength has shown an increase in band depth for higher quantity but more prominent in coal than soil contamination for smaller amount of addition of contamination levels. However, absorption depth at 1000 nm is almost unchanged for soil contamination but reduces for coal contamination. Asymmetry has shown a subtle change for coal than soil contamination. First derivative analysis has depicted a peak shift for soil in visible region whereas it is not observed for coal contamination. Percentage change in reflectance has shown a reduction in reflectance in visible region whereas a reverse pattern of reflectance was observed in SWIR region for soil contamination. The albedo for soil contamination was found to be decreased gradually but coal has shown an exponential decrease for the same amount of contamination level. This study demonstrates that a combination of absorption band depth, asymmetry, first derivative, percentage change in reflectance and albedo could provide useful information over identification/discrimination of soil and coal contamination over snow bound surface.

Acknowledgements

The authors would like to thank Dr R R Navalgund, Director, SAC and Dr J S Parihar, Deputy Director, RESA for their guidance and support during the investigation. They are also thankful to Dr Ajai, Group Director, MESG for his comments and suggestions on the manuscript. Authors would like to acknowledge the help of SASE Team Members during the field investigations.

References

Clark R N and Roush T L 1984 Reflectance spectroscopy: Quantitative analysis techniques for remote sensing applications; *J. Geophys. Res.* **89** 6329–6340.

Gao B, Heidebrecht K B and Goetz A F H 1993 Derivation of scaled surface reflectances from AVIRIS data; *Remote Sens. Environ.* **44** 165–178.

Gerland S, Winther J G, Orbaek J B, Eliston G, Oritsland N A, Blanco A and Ivanov B 1999 Physical and optical properties of snow covering Arctic tundra on Svalbard; *Hydrol. Proc.* **13** 2331–2343.

Hall D K, Riggs G A and Salomonson V V 1995 Development of methods for mapping global snow cover using moderate resolution image spectroradiometer data; *Remote Sens. Environ.* **54** 127–140.

Hall D K, Riggs G A, Salomonson V V, Digiromamo N and Bayer K J 2002 MODIS snow-cover products; *Remote Sens. Environ.* **83** 181–194.

Kulkarni A V, Singh S K, Mathur P and Mishra V D 2006 Algorithm to monitor snow cover using AWiFS data of RESOURCESAT for the Himalayan region; *Int. J. Remote Sens.* **27**(**12**) 2449–2457.

Mohile C M, Pethkar J S and Deshpande N R 2004 *Climatic variability over Western Himalaya*; Proceedings International Symposium on Snow Monitoring and Avalanches (ISSMA-2004), pp. 171–200.

Negi H S, Kulkarni A V and Singh S K 2006 Effect of contamination and mixed objects on snow reflectance using spectroradiometer in Beas Basin, India; *Proc. SPIE* **6411** 641115, doi: 10.1117/12.693879.

Negi H S, Kulkarni A V and Semwal B S 2009 Study of contaminated and mixed objects snow reflectance in Indian Himalaya using spectroradiometer; *Int. J. Remote Sens.* **30**(**2**) 315–325.

O'Brian H W and Munis H 1975 Red and near-infrared spectral reflectance of snow; *U.S.A. CRREL Research Report* **332**, 18 p.

Osada K, Iida H, Kido M, Matsunaga K and Iwasaka Y 2004 Mineral dust layers in snow at Mount Tateyama, Central Japan: Formation processes and characteristics; *Tellus* **56B** 382–392.

Price J C 1998 An approach for analysis of reflectance spectra; *Remote Sens. Environ.* **64** 316–330.

Singh S K, Negi H S, Babu G R K, Kulkarni A V and Sharma J K 2005 Spectral reflectance investigations of snow and other objects using ASD radiometer; SAC Scientific Note No. RSAM/SAC/RESIPA/MWRG-GLI/SN 23/2005, 43 p.

Singh S K, Negi H S and Kulkarni A V 2008 *Study of snowpack characteristics using field spectroradiometer in Beas basin, H.P.*; Proceedings of International Workshop on Snow, Ice, Glacier and Avalanche, IIT, Mumbai.

Singh S K, Kulkarni A V and Chaudhary B S 2010 Hyperspectral analysis of snow reflectance to understand the effects of contamination and grain size; *Ann. Glaciol.* **51**(**54**) 83–88.

Warren S G and Wiscombe W J 1980 A model for the spectral albedo of snow-II: Snow containing atmospheric aerosols; *J. Atmos. Sci.* **37** 2734–2745.

Wiscombe W J and Warren S G 1981 A model for the spectral albedo of snow-I: Pure snow; *J. Atmos. Sci.* **37** 2712–2733.

MS received 5 May 2010; revised 27 December 2010; accepted 4 January 2011